Optical and Quantum Electronics **26** *(1994) S285–S299*

Design of 1480-nm diode-pumped Er^{3+}-doped integrated optical amplifiers

F. HORST, T. H. HOEKSTRA, P. V. LAMBECK, Th. J. A. POPMA
University of Twente, MESA Research Institute, PO Box 217, NL-7500 AE Enschede, The Netherlands

Received 10 May; revised 30 July; accepted 16 August 1993

Erbium-doped Y_2O_3 integrated optical amplifiers are designed for low-threshold operation and 3 dB amplification. The most important design parameter for minimal threshold, the erbium concentration, is found to have an optimum value of 0.35 at% for a given waveguide structure with 1.0 dB cm^{-1} background loss. The corresponding threshold power is 7 mW. The pump power to obtain 3 dB gain is found to be 22 mW for an amplifier with an optimum erbium concentration of 0.6 at% and 2.8 cm length. At 30 mW pump power the maximum gain is shown to be 5 dB.

Designing is done using a comprehensive numerical model of an erbium-doped integrated optical amplifier. In the model two-dimensional intensity-dependent overlap integrals are used, which allow arbitrary erbium dopant profiles and waveguide cross-sections. Concentration-dependent effects such as quenching and upconversion are also included in the model.

Input parameters for the model are determined from measurements on an unoptimized Er : Y_2O_3 optical waveguide amplifier. Amplification simulations and gain measurements of the unoptimized waveguides are found to be in close agreement, providing a sound basis for the design calculations.

1. Introduction

Currently there is a lot of interest in erbium-doped integrated optical amplifiers for the third window of telecommunication near 1.5 μm, reasons including their small size, potential integration with light sources and receivers and the use of amplifying waveguides as a loss-compensating component in waveguides and splitters.

There are several reports on the fabrication of erbium-doped optical waveguides, for example [1–6], but only in a few cases has amplification been demonstrated [7–11]. Apart from the fabrication, design is important to create efficient erbium-doped optical amplifiers. To design an erbium-doped amplifier an appropriate model describing the behaviour of the amplifier is required. Extensive modelling has been done for erbium-doped fibre amplifiers [12–14] but in general these models cannot be applied directly to integrated optical waveguides. Major differences between integrated optical amplifiers and fibre amplifiers are high erbium concentrations leading to ion–ion interactions, high background loss that may not be

0306–8919

neglected, and noncircular waveguide modes and erbium distributions. Models including some of these aspects have been reported [15–19] and show that the erbium concentration is the key parameter in designing integrated optical amplifiers.

We have developed a numerical propagation model for erbium-doped integrated optical amplifiers that combines most of these aspects; for example, mode profile calculated by the Marcatili method, intensity-dependent overlap integrals, background losses, concentration-dependent lifetime and upconversion. The necessary input parameters for the model are experimentally determined from an unoptimized $Er : Y_2O_3$ integrated optical waveguide [20]. Comparison of the measured and calculated gain characteristics provides a validity check of the model.

This paper describes the design of a 1480 nm diode laser-pumped integrated optical amplifier using this comprehensive model. The use of laser diode pumping promises a high degree of integration and small packaging but also involves relatively low pump powers. Therefore, a low threshold pump power is an important design parameter. Using the measured parameters and the propagation model, an $Er : Y_2O_3$ optical amplifier with minimal threshold for 1480 nm diode pumping is designed. In addition, the design of 3 dB amplifiers for application in lossless splitters is evaluated and the maximum achievable gain at moderate pump powers is examined.

2. Propagation model

In this section a model is developed to predict the amplification of a signal at 1535 nm wavelength in erbium-doped waveguides pumped at 1480 nm. The numerical propagation model is based on a three-level system. The field profiles of a ridge-type optical waveguide are evaluated by the Marcatili method [21] and the overlap integrals are regarded as being intensity-dependent. The background attenuation of the waveguide is taken into account during propagation. Also, concentration-dependent ion–ion interactions, such as quenching and two-photon upconversion, are incorporated in the model.

We used the 1480 nm pump band to excite the erbium ions because this wavelength shows almost no excited state absorption (ESA) [22], low amplified spontaneous emission (ASE), low background loss and good modal overlap between pump and signal. In our model we have therefore not included ESA and ASE. Other effects we do not consider in our model are three-photon upconversion, erbium concentration gradient in the propagation direction, and nonlinear refractive index. A disadvantage of direct band pumping with 1480 nm is that this wavelength also partly depopulates the excited state by stimulated emission, so that complete population inversion is impossible.

2.1. Amplification in a uniform medium

In a uniform erbium-containing medium, erbium atoms are excited by the 1480 nm pump beam from the $^4I_{15/2}$ ground state to the upper part of the $^4I_{13/2}$ band. Then they relax to the lower part of this band, which serves as the starting point for the stimulated transition back to the ground state. The simplified three-level system and the transitions that we used to describe this process are shown in Fig. 1. The system is irradiated by a pump photon flux ϕ_p and a signal photon flux ϕ_s (both in number of photons per m^2 per s). These photon fluxes are related to the intensity I of the light by $\phi = I/h\nu$.

The formulation and solving of the rate-equations for this system in CW operation are straightforward [12]. Assuming that the decay rate T_{32} from level 3 to level 2 is very large compared to the other time constants in the system and that the influence of the signal photon

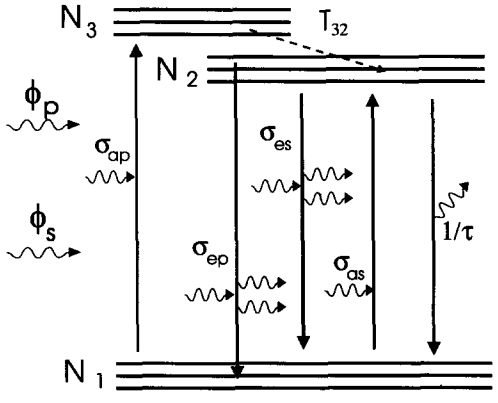

Figure 1 Simplified three-level system for erbium.

flux on the population can be neglected, which is true when the situation close to threshold is considered, the system can be regarded as a quasi two-level system. The following populations can then be found:

$$N_2 = N\frac{\sigma_{ap}\phi_p}{(\sigma_{ap}+\sigma_{ep})\phi_p + 1/\tau} \tag{1}$$

$$N_1 = N\frac{\sigma_{ep}\phi_p + 1/\tau}{(\sigma_{ap}+\sigma_{ep})\phi_p + 1/\tau} \tag{2}$$

where N, N_1 and N_2 are total, ground-state and excited-state densities of erbium atoms, respectively, the σ's are transition cross-sections as defined in Fig. 1, and τ is the radiative lifetime of the excited level.

After propagating a distance $\mathrm{d}z$ through an erbium-containing medium, the change $\mathrm{d}\phi$ of a photon flux ϕ is given by

$$\mathrm{d}\phi = (\alpha - \gamma)\phi\,\mathrm{d}z \tag{3}$$

Here, α and γ are the amplifying and attenuating contributions, respectively, of the erbium ions. From the transitions in Fig. 1 we find

$$\begin{aligned} \alpha_s &= \sigma_{es}N_2 \qquad \gamma_s = \sigma_{as}N_1 \\ \alpha_p &= \sigma_{ep}N_2 \qquad \gamma_p = \sigma_{ap}N_1 \end{aligned} \tag{4}$$

2.2. Amplification in a waveguide

In a waveguide (oriented along the z-axis), the photon fluxes depend on the x-, y- and z-coordinates in the waveguide. The distribution of the active erbium atoms may depend upon the x- and y-coordinates across the waveguide. From Equations 1 and 4, a position-dependent amplification and attenuation is found:

$$\alpha_s(x,y,z) = \sigma_{es}N(x,y)\frac{\sigma_{ap}\phi_p(x,y,z)}{(\sigma_{ap}+\sigma_{ep})\phi_p(x,y,z) + 1/\tau} \tag{5}$$

In the limit of low amplification, which holds when the model is used for threshold calculations, the normalized distribution of the photon flux ($M(x,y)$) across the waveguide is

completely determined by waveguide geometry, refractive indexes and wavelength. We assumed that all pump and signal power propagates in the fundamental TE_{00} waveguide mode. While light propagates along the waveguide, only the total modal photon flux (ϕ_m) through the waveguide will vary with z-position. Therefore we can write:

$$\begin{aligned} \phi_p(x,y,z) &= \phi_{mp}(z)M(x,y) \\ \phi_s(x,y,z) &= \phi_{ms}(z)M(x,y) \end{aligned} \tag{6}$$

The photon flux distribution $M(x,y)$ can be taken approximately as being equal for pump and signal because the wavelengths are close together and the waveguide dispersion is low in the region around 1.5 μm. To calculate the distribution of the photon flux, a method derived from Marcatili's field shadow method is used [21].

The distribution of the erbium atoms is taken as z-independent:

$$N(x,y) = N_{\mathrm{Er}} D(x,y) \tag{7}$$

The function $D(x,y)$ describes the distribution of the erbium atoms across the waveguide. This function is normalized to the maximum of the concentration of the erbium atoms.

In a waveguide, the propagating mode is amplified or attenuated as a whole. The modal amplification of the signal light ($\alpha_{ms}(z)$) is equal to the overlap-integral of the position-dependent amplification ($\alpha_s(x,y,z)$) and the signal beam ($\phi_s(x,y,z)$):

$$\alpha_{ms}(z) = \frac{\iint \alpha_s(x,y,z)\phi_s(x,y,z)\,\mathrm{d}y\,\mathrm{d}x}{\iint \phi_s(x,y,z)\,\mathrm{d}y\,\mathrm{d}x} \tag{8}$$

The expressions for the attenuation of signal light and the amplification and attenuation of pump light are similar.

Combining Equations 5, 6, 7 and 8 yields

$$\alpha_{ms}(z) = N_{\mathrm{Er}}\sigma_{es}Q\mathcal{S}(B\cdot\phi_{mp}(z)) \tag{9}$$

$$\gamma_{ms}(z) = N_{\mathrm{Er}}\sigma_{as}[\mathcal{C} - Q\mathcal{S}(B\cdot\phi_{mp}(z))] \tag{10}$$

$$\alpha_{mp}(z) = N_{\mathrm{Er}}\sigma_{ep}Q\mathcal{S}(B\cdot\phi_{mp}(z)) \tag{11}$$

$$\gamma_{mp}(z) = N_{\mathrm{Er}}\sigma_{ap}[\mathcal{C} - Q\mathcal{S}(B\cdot\phi_{mp}(z))] \tag{12}$$

with

$$Q = \sigma_{ap}/(\sigma_{ep} + \sigma_{ap}) \tag{13}$$

$$B = (\sigma_{ep} + \sigma_{ap})\tau \tag{14}$$

and the overlap integrals

$$\text{'Confinement'}: \quad \mathcal{C} = \iint D(x,y)M(x,y)\,\mathrm{d}y\,\mathrm{d}x \tag{15}$$

$$\text{'Saturating overlap'}: \quad \mathcal{S} = \iint \frac{D(x,y)M(x,y)^2}{M(x,y) + 1/(B\cdot\phi_{mp}(z))}\,\mathrm{d}y\,\mathrm{d}x \tag{16}$$

2.3. Ion–ion interactions

An important modelling parameter for erbium-doped integrated optical amplifiers is the erbium concentration. In order to achieve a significant gain per unit length, relatively high erbium

concentrations are needed in comparison with fibre amplifiers, because of the short length of common integrated optic devices. At these high erbium concentrations, energy transfer processes between neighbouring erbium ions influence the population densities. Modelling of high-concentration erbium-doped optical amplifiers should account for these effects.

When the erbium ions are close enough to show coupling by Coulomb or exchange interactions, referred to as ion–ion interactions, the energy of an excited ion can be transferred nonradiatively to another ion. Because identical ions are involved, the energy transfer of the excited state is resonant, yielding a rapid migration of the excitation energy. This is known as exciton transfer [25]. Among possible depopulation mechanisms of the excited state are quenching of the exciton and upconversion processes, both of which will be included in the model.

Quenching of the excited state leads to a reduced lifetime by introducing an additional decay channel. The quenching rate depends on the exciton migration and the number and properties of the quenching centres. The energy migration can be described by a diffusion process, where either a diffusion-limited or a fast diffusion case can be distinguished [24, 25]. The concentration-dependent luminescent lifetime τ can be written as

$$\tau^{-1} = \tau_0^{-1} + \tau_D^{-1} \tag{17}$$

where

$$\tau_D^{-1} = q_1 \cdot N_{\mathrm{Er}} \qquad \text{(fast diffusion)} \tag{18}$$

$$\tau_D^{-1} = q_2 \cdot N_{\mathrm{Er}}^2 \qquad \text{(diffusion limited)} \tag{19}$$

The lifetime of an isolated ion is given by τ_0, and q_1 and q_2 are coefficients related to the ion–ion transfer probability.

In Section 3 it will be shown that Y_2O_3 corresponds to the fast diffusion case, whereas YAG, for example, which is a known strong-quenching material, follows the diffusion limited case [24].

Besides quenching, upconversion [26] can also result in a nonamplifying transition from the excited state. In the case of stepwise upconversion, the energy transfer of two excited ions results in excitation of a higher energy level. Because two excited ions are involved, the upconversion rate is proportional to $k_2 N_2^2$, where k_2 is an upconversion constant [18, 23]. Inclusion of this transition in the rate equations results in a quadratic expression for the populations. Solving these equations for the steady-state condition yields a modifying factor to be included in the saturating overlap integral:

$$\mathcal{S} = \int\int \frac{D(x,y)M(x,y)^2}{M(x,y) + 1/(B \cdot \phi_{mp}(z))} \times \frac{-1 + \sqrt{1 + 4F\xi(x,y,z)}}{2F\xi(x,y,z)} \,\mathrm{d}y\,\mathrm{d}x \tag{20}$$

with

$$\xi(x,y,z) = \frac{M(x,y)/(B \cdot \phi_{mp}(z))}{[M(x,y) + 1/(B \cdot \phi_{mp}(z))]^2} \tag{21}$$

$$F = \frac{k_2 N_{\mathrm{Er}} \sigma_{ap} \tau}{\sigma_{ep} + \sigma_{ap}} \tag{22}$$

2.4. Propagation along the waveguide

The differential equation (3) can be transformed to

$$\phi_{mp}(z + \delta z) = \phi_{mp}(z) \exp\left([\alpha_{mp}(z) - \gamma_{mp}(z) - \gamma_{bkg}]\delta z\right) \tag{23}$$

$$\phi_{ms}(z + \delta z) = \phi_{ms}(z) \exp\left([\alpha_{ms}(z) - \gamma_{ms}(z) - \gamma_{bkg}]\delta z\right) \tag{24}$$

Here, apart from the erbium-related α_m and γ_m, a background attenuation constant γ_{bkg} is introduced to account for waveguide losses caused by, for example, scattering. Equations 23 and 24 can be solved simultaneously using a beam propagation method, starting from the given ϕ_{mp} and ϕ_{ms} at $z = 0$.

For given waveguide geometry, erbium distribution and wavelengths, the overlap integrals in Equations 15 and 20 depend only on the value of $B \cdot \phi_{mp}$ and F. Before computing the beam propagation through the waveguide, the overlap integrals are precalculated for a number of values of $B \cdot \phi_{mp}$ and F. When doing the beam propagation calculations, the values of the integrals are found from the precalculated data by interpolation. In this way, the beam propagation calculations can be repeated for different values of all amplifier parameters except geometry, erbium distribution and wavelengths, without having to repeat the time-consuming overlap calculations.

2.5. Comparison of the propagation model and analytical results

As a consistency check, the results of the propagation model are compared to those of an analytical solution of Equations 23 and 24 [12] that can be found when background losses and ion–ion interactions are neglected and when the intensity of pump and signal light is assumed to be constant across the active region of the waveguide. This second condition is approximately fulfilled when the active atoms are confined to a region around the centre of the waveguide. For the comparison, the amplifier parameters were chosen to duplicate the parameters used in [12]. These parameters are listed in Table I.

Using both models, the gain as a function of waveguide length is calculated for pump powers of 0.5, 1, 1.5 and 2 mW. The resulting curves are shown in Fig. 2. In this figure, the saturation parameter s is used as a fit parameter in the analytical model. A fit value of $s = 6.9 \times 10^{14}\,\mathrm{m^{-1}\,s^{-1}}$ is found.

In the analytical model, the saturation parameter should be calculated from amplifier parameters [12]: $s = A_{\mathrm{eff}} \cdot N_{\mathrm{Er}}/\tau = 7.1 \times 10^{14}\,\mathrm{m^{-1}\,s^{-1}}$. The small difference between the calculated saturation parameter and the saturation parameter fitted to allow the analytical model duplicate the propagation model results is probably due to the intensity of pump and signal light not being constant across the active region of the waveguide, leading to slightly different behaviour of the propagation model.

TABLE I Parameters used in the comparison of the analytical and the propagation model

Waveguide geometry	See Fig. 3, but with erbium confined to a central area $A_{\mathrm{eff}} = 4.2 \times 0.5\,\mu\mathrm{m}^2$
Resulting confinement	$\mathcal{S} = 0.6$
Waveguide length	$l = 50\,\mathrm{m}$
Pump wavelength	$\lambda_p = 1480\,\mathrm{nm}$
Pump absorption cross-section	$\sigma_{ap} = 1.85 \times 10^{-25}\,\mathrm{m}^2$
Pump emission cross-section	$\sigma_{ep} = 5.77 \times 10^{-26}\,\mathrm{m}^2$
Signal wavelength	$\lambda_s = 1535\,\mathrm{nm}$
Signal absorption cross-section	$\sigma_{as} = 3.0 \times 10^{-25}\,\mathrm{m}^2$
Signal emission cross-section	$\sigma_{es} = 4.15 \times 10^{-25}\,\mathrm{m}^2$
Erbium concentration	$N_{\mathrm{Er}} = 1.0 \times 10^{25}\,\mathrm{m}^{-3}$
Erbium radiative lifetime	$\tau = 10\,\mathrm{ms}$
Saturation parameter, calculated	$s = A_{\mathrm{eff}} \cdot N_{\mathrm{Er}}/\tau = 7.1 \times 10^{14}\,\mathrm{m^{-1}\,s^{-1}}$
Saturation parameter, from fit	$s = 6.9 \times 10^{14}\,\mathrm{m^{-1}\,s^{-1}}$

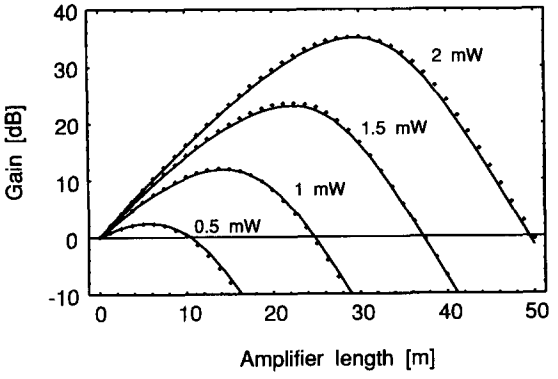

Figure 2 Gain as a function of waveguide length, calculated using both the analytical (dotted lines) and the propagation model (continuous lines). Pump powers of 0.5, 1, 1.5 and 2 mW were used.

3. Experiments

The design of a realistic erbium-doped integrated optical amplifier requires first the determination of material and waveguide parameters. We therefore fabricated waveguiding structures based on Er : Y_2O_3 films. Y_2O_3 is used as host material for the erbium ions because of its high infrared transparency, high refractive index, high potential for rare-earth incorporation, low phonon energy, good physical and chemical properties and the possibility of thin film deposition. Polycrystalline columnar Er : Y_2O_3 thin optical films were deposited on oxidized silicon substrates by reactive sputtering using sputterguns [20]. Ridge channel waveguides were formed by photolithography and ion beam sputter etching of these films.

3.1. Er : Y_2O_3 waveguide parameters

Refractive index and thickness of the Er : Y_2O_3 and SiO_2 layers were determined from prism coupling experiments [28]. The ridge step height was measured by a surface profiler and the channel width was determined with a microscope. A typical waveguide cross-section is shown in Fig. 3 including the TE_{00} mode profile as calculated by the Marcatili method [21].

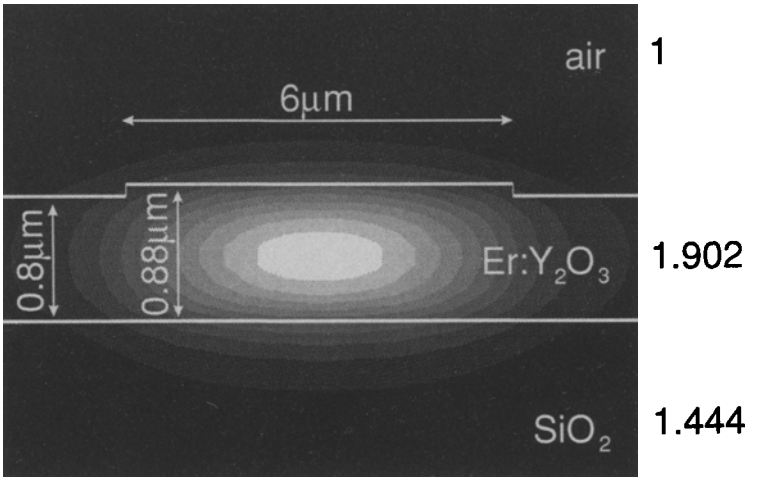

Figure 3 Cross-section of erbium waveguide, with TE_{00} mode profile.

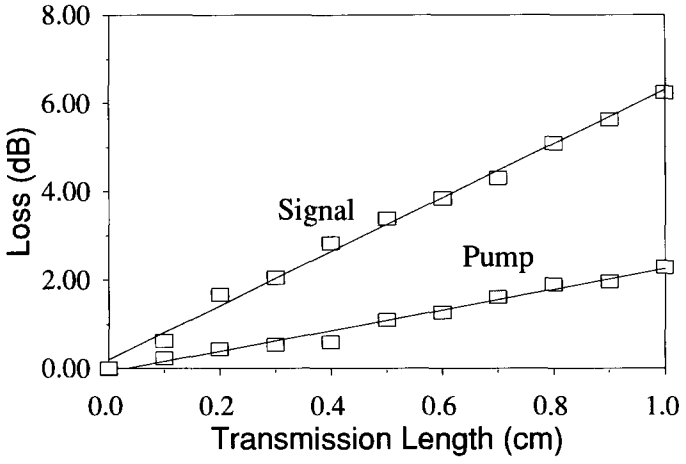

Figure 4 Attenuation $\gamma_{bkg} + \gamma_{Er}$ of pump and signal light in the waveguide.

Absorption cross-sections σ_{ap}, σ_{as} are calculated from the modal attenuation γ_m due to the erbium ions by $\sigma_a = \gamma_m/(\mathcal{C} \cdot N_{Er})$. This relation can be found from Equations 10 and 12 in the limit of low pump power. $\mathcal{C}$ is the overlap integral between the optical mode and the erbium ions as defined in Equation 15. The erbium ion density N_{Er} was determined by RBS measurements. The total attenuation $\gamma = \gamma_{bkg} + \gamma_m$ of a waveguide was determined by end-coupling a light beam in the channel waveguide and coupling out the light at various transmission lengths. A representative example of attenuation measurements of pump and signal beam is shown in Fig. 4. The background attenuation γ_{bkg} can be estimated either from attenuation measurements of undoped Y_2O_3 waveguides or from an attenuation measurement at a wavelength just beside the erbium absorption band.

The emission cross-sections were determined from the absorption cross-sections by the

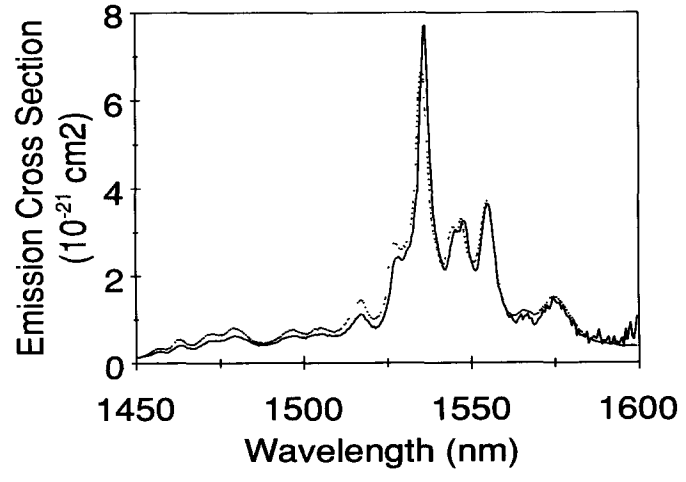

Figure 5 Emission cross-sections obtained by both the McCumber (solid line) and the Fuchtbauer–Ladenburg method (dotted line).

reciprocity or McCumber method [29, 30]. To check the reciprocity method, emission cross-sections are also calculated from the luminescence spectra by the Fuchtbauer–Ladenburg method [29]. The results of both methods compare well, except for the peak wavelength, as shown in Fig. 5.

The luminescence lifetime was determined from the fast exponential component of the time response decay of guided luminescence to an excitation pulse. In order to determine the concentration dependence of the luminescence lifetime, we performed lifetime measurements for optical waveguides with various erbium concentrations as shown in Fig. 6. Whereas the measured luminescence decay rate varies linearly with the erbium concentration, the concentration dependence can be modelled by fast diffusion: $1/\tau = 1/\tau_0 + q_1 \cdot N_{\mathrm{Er}}$. A fit to this model gives $\tau_0 = 10.4$ ms, which is used as the radiative lifetime in the Fuchtbauer–Ladenburg analysis.

The upconversion coefficient k_2 can be determined from the nonexponential luminescence decay of the first excited state [27], or from the two-photon upconverted luminescence [23], or from gain measurements [16]. In all these cases the upconversion coefficient is determined by matching of simulations to measurements, where the upconversion coefficient serves as a fit parameter. In the next section the upconversion coefficient is obtained from comparison of gain measurements with our simulations.

3.2. Optical amplifier measurements

In order to check the model with experimental data, an unoptimized Er : Y_2O_3 optical amplifier was fabricated. The parameters of this amplifier, measured as detailed in Section 3.1, are listed in Table II.

Both by experiment and from the propagation model, the gain in this waveguide was obtained as a function of pump power. As a pump source a 1480 nm pigtailed laser diode was used, with a maximum of 30 mW coupled into the fibre. The pump power was launched into the integrated optical amplifier with an efficiency of 7%. The resulting curves are drawn together in Fig. 7. The pumped waveguides show a clear luminescence at 980 nm and 554 nm, demonstrating two-photon upconversion and also indicating that three-photon processes occur.

In the model calculations the upconversion coefficient k_2 was used to fit the simulation results to the experimental curve. The obtained fit value of $k_2 = 0.25 \times 10^{-23}\ \mathrm{m^3\,s^{-1}}$ is of

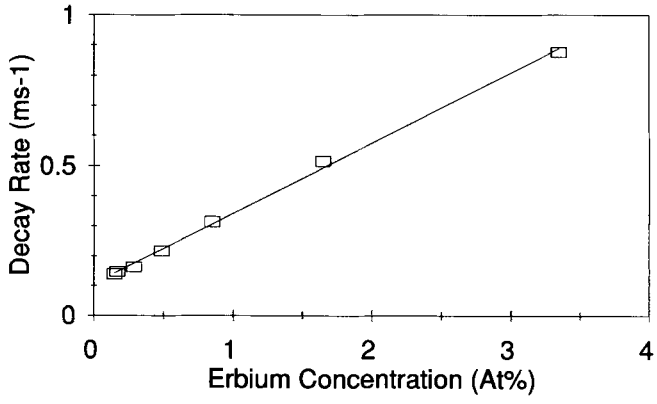

Figure 6 Decay rate $1/\tau$ of erbium as a function of erbium concentration.

TABLE II Waveguide parameters of the experimental optical amplifier

Waveguide geometry	See Fig. 3
Waveguide length	$l = 39\,\text{mm}$
Pump wavelength	$\lambda_p = 1480\,\text{nm}$
Pump absorption cross-section	$\sigma_{ap} = 1.4 \times 10^{-25}\,\text{m}^2$
Pump emission cross-section	$\sigma_{ep} = 4.5 \times 10^{-26}\,\text{m}^2$
Signal wavelength	$\lambda_s = 1535\,\text{nm}$
Signal absorption cross-section	$\sigma_{as} = 5.5 \times 10^{-25}\,\text{m}^2$
Signal emission cross-section	$\sigma_{es} = 5.5 \times 10^{-25}\,\text{m}^2$
Erbium concentration	$N_{\text{Er}} = 0.34\,\text{at\%}\ (2.3 \times 10^{-23}\,\text{cm}^{-3})$
Erbium distribution	See Fig. 3
Erbium radiative lifetime	$\tau = 10\,\text{ms}$
Estimated background attenuation	$\gamma_{bkg} = 1.0\,\text{dB cm}^{-1}$
Estimated upconversion coefficient	$k_2 = 0.25 \times 10^{-23}\,\text{m}^3\,\text{s}^{-1}$

the same order of magnitude as the reported values of the upconversion coefficient of erbium-doped YAG ($1.5 \times 10^{-23}\,\text{m}^3\,\text{s}^{-1}$) [27]. The value of k_2 depends considerably on the value of the background attenuation γ_{bkg} used in the simulations. Whereas the background loss is determined with an uncertainty of about 15%, the upconversion coefficient k_2 will show at least the same error.

4. Design

When designing a waveguide amplifier, several goals can be set, depending on the application of the optical amplifier. Design objectives considered in this section are:

Low threshold power, i.e. minimum pump power required to overcome the background losses and so produce a virtually lossless waveguide.
3 dB gain. This is interesting for application in lossless integrated optic splitters.
Maximum gain at minimum pump power, which is important for use as a power amplifier.

In this section optimum values will be determined for waveguide length, erbium concentration and pump power, to achieve the proposed design goals. The amplifier geometry is

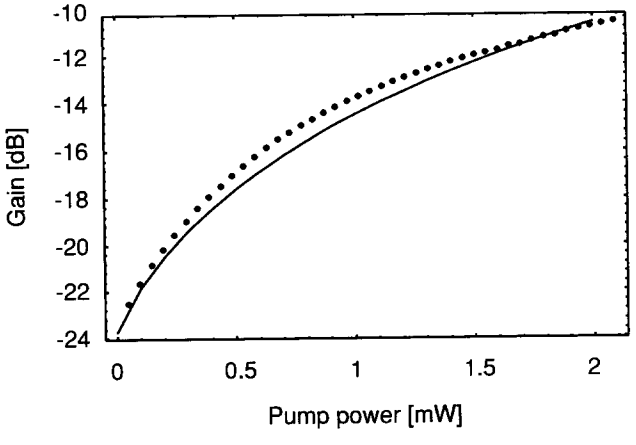

Figure 7 Gain in unoptimized waveguide amplifier. Dotted curve, experimental result; continuous line, model calculation.

not varied because it has to be considered in relation to other aspects besides the amplifying characteristics. For example, waveguide width and thickness are related to the coupling efficiency of the pump power into the integrated optical amplifier and influence ordinary waveguiding properties, which are often determined by the utilization of the amplifier. However, the rather high refractive index and low film thickness of the Y_2O_3 waveguiding layer used in the design already result in a relative high intensity of the guided modes. The dopant distribution is also kept constant, because at the moment it is predetermined by the waveguiding layer owing to technological constraints.

The other input parameters of the model will be taken as measured in Section 3 and are listed in Table II.

Constraints that will be used in the designing process are the maximum available pump power of 30 mW of our diode pump laser and a maximum length of 6 cm of the waveguide, which is the maximum length of a straight waveguide we can reach on a 3 inch diameter silicon wafer. Also, we will only consider the use of pumping at 1480 nm wavelength.

4.1. Calculations

In Fig. 8 the calculated gain as a function of waveguide length is shown for an imaginary amplifier where the effects of background losses and exciton transfer processes are neglected. The figure shows a trade-off between optimum waveguide length and erbium concentration, because lower erbium concentrations require longer waveguides to develop the maximum gain. However, the actual value of the maximum gain is independent of erbium concentration. Likewise, the threshold pump power of this imaginary waveguide amplifier is independent of erbium concentration. The threshold power is taken as the pump power that results in 0 dB net amplification at the very beginning of the waveguide.

In further threshold calculations, background losses and exciton transfer processes are included. The results shown in Fig. 9 now indicate a clear optimum erbium concentration exists for minimum threshold power. At low erbium concentrations, the background losses reduce the maximum gain in the long waveguides that are required. On the other hand, high erbium concentrations lead by intensified exciton transfer processes to a reduction of the life-

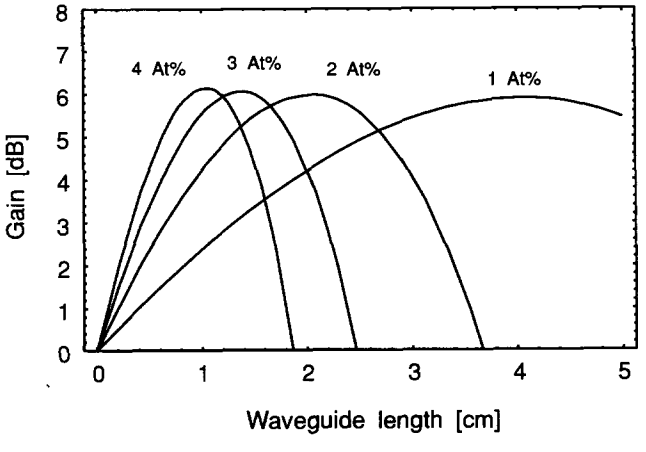

Figure 8 Gain in 1.5 mW pumped erbium waveguide for various erbium concentrations, when background losses and lifetime reduction due to exciton transfer processes are neglected.

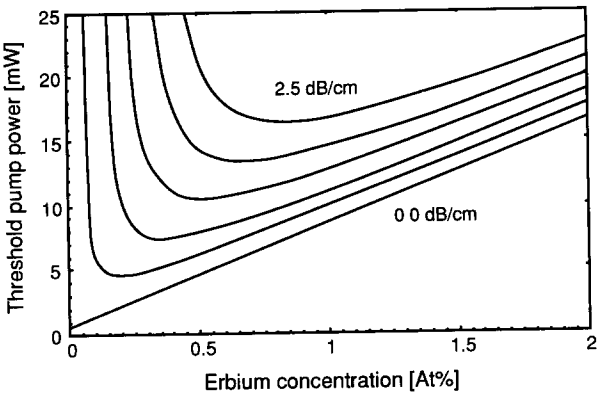

Figure 9 Amplifier threshold pump power as a function of erbium concentration. Curves are drawn for background losses of $\gamma_{bkg} = 0.0$, 0.5, 1.0, 1.5, 2.0 and 2.5 dB cm^{-1}.

time of excited erbium atoms and increased upconversion (see Fig. 6), again resulting in reduction of the maximum gain. The threshold calculations in Fig. 9 are repeated for six values of the background losses from 0.0 to 2.5 dB cm^{-1}. For lower background losses a lower optimum erbium concentration is found because a slower development of the accumulated gain in the waveguide is allowed. The erbium concentration may then be lower, avoiding gain degradation by ion–ion interactions.

The large effect of the exciton transfer processes on the threshold pump power is illustrated by the threshold curve in absence of background loss in Fig. 9. It can be seen that the threshold pump power increases from 1.5 mW for 0.1 at% erbium to 16 mW for 2 at% erbium concentration. Not only the higher threshold, but also the drastic decrease of the gain due to the appearance of ion–ion interactions, can be observed [18]. For example, Fig. 8 shows a gain of 6 dB for 1.5 mW pump power, an amplifier of 4 cm length, 1.0 at% erbium concentration and no ion–ion interactions or background losses, whereas Fig. 9 indicates that for the same amplifier, including ion–ion interactions, 0 dB threshold is reached at 8 mW pump power.

The first main design problem – optimization of the waveguide for minimum threshold pump power – can be dealt with using Fig. 9. From our measurements we estimated the background loss of the waveguide to be approximately 1.0 dB cm^{-1}. From Fig. 9 it can be concluded that the expected threshold power in this waveguide is $\approx$7 mW at an optimum erbium concentration of $\approx$0.35 at%.

Figures 10 and 11 are useful in determining the optimum erbium concentration and waveguide length to meet the 3 dB design objective, again for waveguides with a background loss of 1.0 dB cm^{-1}. The same figures can be used to obtain the maximum gain in a waveguide with optimal length and erbium concentration for the given pump power limit of 30 mW. Figure 10 shows the gain as a function of the erbium concentration for pump powers in the range of 10 to 30 mW for the corresponding optimal amplifier length. This optimal length can be deduced from Fig. 11, where the gain as a function of waveguide length is shown for pump powers in the range of 10 to 30 mW and an erbium concentration of 0.6 at%.

From Fig. 10 it follows that a gain of 3 dB is obtained when approximately 22 mW pump power is used at an optimum erbium concentration of $\approx$0.6 at%. The optimum length in this case is $\approx$2.8 cm, as can be seen from Fig. 11.

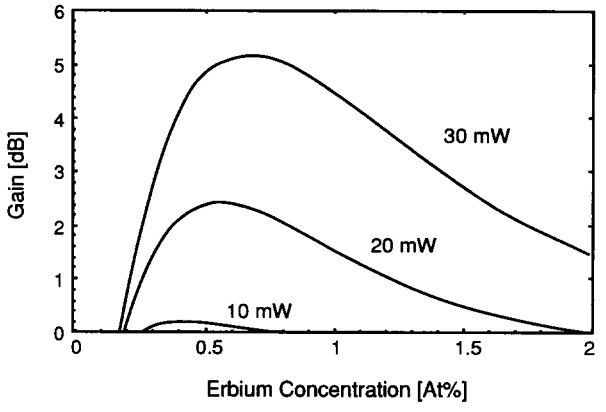

Figure 10 Maximum amplifier gain as a function of erbium concentration. The waveguide length is optimized. Curves are drawn for 10, 20 and 30 mW pump power. $\gamma_{bkg} = 1.0\,\mathrm{dB\,cm^{-1}}$.

For 30 mW pump power a maximum gain of ≈5 dB is obtained from Fig. 10 at an optimum erbium concentration of ≈0.7 at% and an optimum waveguide length of 4 cm (see Fig. 11).

5. Conclusions and discussion

Erbium-doped Y_2O_3 integrated optical amplifiers are designed using a comprehensive numerical model. The propagation model presented, based on a three-level system, evaluates the gain of erbium-doped integrated optical amplifiers for arbitrary erbium dopant profiles and waveguide cross-sections. Special features of the model include two-dimensional intensity-dependent overlap integrals, background losses, concentration-dependent lifetime and two-photon upconversion processes. The model does not include ASE, ESA, three-photon upconversion processes or nonlinear refractive indices. However, the results of the propagation model are in good agreement with the gain measurements of Er : Y_2O_3 integrated optical amplifiers, showing that the model developed is a dependable tool in the design process. All input parameters for the model are experimentally determined from reactive-sputtered Er : Y_2O_3 optical waveguides, except for the upconversion coefficient k_2, which was obtained by matching with the gain measurements.

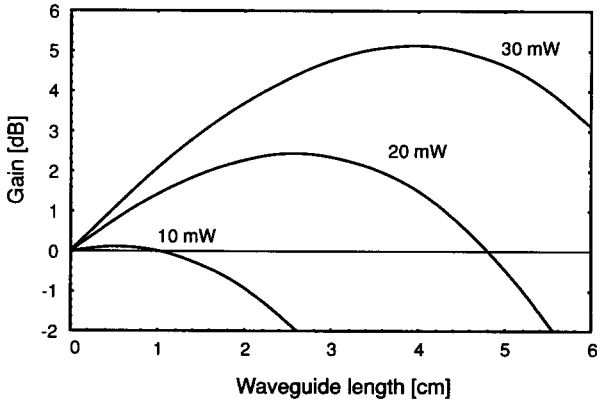

Figure 11 Gain as a function of amplifier length. $\gamma_{bkg} = 1.0\,\mathrm{dB\,cm^{-1}}$, $N_{Er} = 0.6$ at%. Curves are drawn for 10, 20 and 30 mW pump power.

The main objective of the design study on Er : Y_2O_3 integrated optical amplifiers was the optimization of the amplifier with respect to the threshold power at a pump wavelength of 1480 nm. A low threshold pump power enables laser diode pumping of the integrated optical amplifier.

The amplifier gain is examined as a function of amplifier length, background loss, erbium concentration and pump power for a given waveguide geometry and erbium distribution. Calculations predict a minimal threshold of 7 mW for an amplifier with 0.35 at% erbium concentration and a background loss of 1.0 dB cm^{-1}. Application of the amplifying characteristics to produce lossless splitters requires minimal 3 dB gain, which is achieved for 22 mW pump power, an erbium concentration of 0.6 at%, an amplifier length of 2.8 cm and a background loss of 1.0 dB cm^{-1}. For 30 mW pump power a maximum gain of 5 dB is found for an amplifier with an optimum erbium concentration of 0.7 at%, an optimum length of 4 cm and a background loss of 1.0 dB cm^{-1}.

The numerical model predicts only moderate amplifier gains for pump powers available from laser diodes, which is not sufficient for application as a power amplifier. Therefore, the presented erbium-doped integrated optical amplifier has to be further optimized and tailored to obtain satisfactory amplification. Lower threshold and higher gains can, for example, be achieved by: (1) Reducing the background losses of the erbium doped waveguides. A threshold of 5 mW is expected for a background loss of 0.5 dB cm^{-1}, which should be possible for Er : Y_2O_3 waveguides using improved fabrication techniques. (2) Maximizing the modal pump intensity by using optimal waveguide dimensions. However, smaller dimensions also reduce the coupling efficiency of the pump power into the amplifier. (3) Matching of the optical fields with the erbium dopant profile. This requires a graded distribution of the erbium dopant, which can easily be achieved by the applied fabrication method of the Er : Y_2O_3 waveguides.

However, efficient pumping, possibly even for optimized amplifiers, needs a rather high erbium concentration for integrated optical amplifiers of a few centimetres length. At these high erbium concentrations the gain is significantly reduced by ion–ion interactions. Sensitizing with ytterbium [26] to improve the pump efficiency might be the most promising way to obtain efficient high-gain erbium-doped integrated optical amplifiers.

References

1. A. POLMAN, D C JACOBSON, D J EAGLESHAM, R. C. KISTLER and J M POATE, *J. Appl. Phys.* **70** (1991) 3778.
2. M. M. ABOUELLEIL, G. A. BALL, W. L. NIGHAN and D. J OPAL, *Opt. Lett.* **16** (1991) 1949.
3. R BRINKMANN, W SOHLER and H. SUCHE, *Electron. Lett.* **27** (1991) 415.
4. T. KITAGAWA, K. HATTORI, M SHIMIZU, Y. OHMORI and M KOBAYASHI, *Electron Lett.* **27** (1991) 334.
5. X. H. ZHENG and R. J. MEARS, *Appl. Phys. Lett.* **62** (1993) 793.
6. T. H HOEKSTRA, L T H HILDERINK, P V LAMBECK and Th. J POPMA, *Opt. Lett.* **17** (1992) 1506.
7. T KITAGAWA, K. HATTORI, K. SHUTO, M YASU, M. KOBAYASHI and M. HORIGUCHI, *Electron. Lett.* **28** (1992) 1818.
8. W. J WANG, S. I NAJAFI, S. HONKANEN, Q HE, C. WU and J. GLINSKI, *Electron. Lett.* **28** (1992) 1872.
9. J. SCHMULOVICH, A. WONG, Y H. WONG, P C BECKER, A. J. BRUCE and R ADAR, *Electron. Lett.* **28** (1992) 1181.
10. K. SHUTO, K. HATTORI, T KITAGAWA, Y OHMORI and M. HORIGUCHI, *Electron. Lett.* **29** (1993) 139.
11. K HATTORI, T KITAGAWA, M. OGUMA, M. WADA, J. TEMMYO and M. HORIGUCHI, *Electron. Lett.* **29** (1993) 357.
12. C. R GILES and E. DESURVIRE, *J. Lightwave Technol.* **9** (1991) 271.
13. E DESURVIRE, J. L. ZYSKIND and C. R GILES, *J. Lightwave Technol.* **8** (1990) 1730.
14. B. PEDERSEN, A. BJARKLEV, J. H POVLSEN, K DYBDAL and C C LARSEN, *J. Lightwave Technol.* **9** (1991) 1105.
15. S. HELMFRID and G. ARVIDSSON, *IEEE Photon. Technol. Lett.* **2** (1991) 635.
16. O. LUMHOLT, T. RASMUSSEN and A. BJARKLEV, *Electron. Lett.* **29** (1993) 495.

17. T. RASMUSSEN, O. LUMHOLT, J. H. POVLSEN and A. BJARKLEV, *Electron. Lett.* **29** (1993) 455.
18. M. FEDERIGHI, I. MASSAREK and P. F TRWOGA, *IEEE Photon. Technol. Lett.* **5** (1993) 227.
19. W. SOHLER, in *Waveguide Optoelectronics*, edited by J. H. Marsh and R. M. De La Rue (Kluwer Academic Publishers, Dordrecht, 1992) p. 361.
20. T. H. HOEKSTRA, P. V. LAMBECK, H. ALBERS and Th. J. A. POPMA, *Electron. Lett.* **29** (1993) 581.
21. M. A. J. MARCATILI, *Bell Syst. Tech. J.* **48** (1969) 2071.
22. R. J. MEARS and S. R. BAKER, *Opt. Quantum Electron.* **24** (1992) 517.
23. P BLIXT, J. NILSSON, T. CARLNAS and B. JASKORZYNSKA, *IEEE Trans. Photon. Technol. Lett.* **3** (1991) 996.
24. F E. AUZEL, *Radiationless Processes*, edited by B. DiBartolo (Plenum Press, New York, 1979) p. 213.
25. R K. WATTS, in *Optical Properties of Ions in Solids*, edited by B. DiBartolo (Plenum Press, New York, 1974) p. 307.
26. F. E. AUZEL, *Proc. IEEE* **61** (1973) 758.
27. W. Q. SHI, M. BASS and M. BIRNBAUM, *J. Opt. Soc. Am. B* **7** (1990) 1456.
28. R. ULRICH and R. TORGE, *Appl. Opt.* **12** (1973) 2910.
29. S. A PAYNE, L. L. CHASE, L. K. SMITH, W. L. KWAY and W. F KRUPKE, *IEEE J. Quantum Electron.* **28** (1992) 2619.
30. W. J. MINISCALO and R. S. QUIMBY, *Opt. Lett.* **16** (1992) 258.